J Solid State Electrochem (2000) 4: 70–74

ORIGINAL PAPER

S. Durón · R. Rivera-Noriega · M.A. Leyva · P. Nkeng
G. Poillerat · O. Solorza-Feria

Oxygen reduction on a $Ru_xS_y(CO)_n$ cluster electrocatalyst in 0.5 M H_2SO_4

Received: 4 March 1999 / Accepted: 26 May 1999

Abstract A ruthenium-sulfur carbonyl cluster electrocatalyst, $Ru_xS_y(CO)_n$, was synthesized by pyrolysis of $Ru_3(CO)_{12}$ and elemental sulfur in a sealed ampoule at 300 °C. The pyrolyzed compound was characterized by DSC, FT-IR, XRD and SEM (EDX) techniques. The electrocatalytic activity and kinetic parameters for the molecular oxygen reduction were determined by a rotating ring-disk electrode (RRDE) in a 0.5 M H_2SO_4 solution at 25 °C. The cathodic polarization indicates two Tafel slopes: -0.124 ± 0.002 V dec^{-1} at low and -0.254 ± 0.003 V dec^{-1} at high overpotentials, and first-order kinetics with respect to O_2 concentration. From the analysis of Levich plots and RRDE results, the oxygen reduction on $Ru_xS_y(CO)_n$ was determined to proceed mostly via a multielectron transfer path ($4e^-$) to water formation ($>94\%$).

Key words Rotating ring-disk electrode · Oxygen · Reduction · Ruthenium-cluster electrocatalyst · Sulfuric acid

Introduction

Transition-metal carbonyl clusters are an important area in organometallic chemistry research. In particular, ruthenium and osmium clusters have been extensively studied because of their good balance between reactivity and stability [1–5]. The preparation of supported metal clusters by decarboxylation of metal carbonyl clusters is exemplified by the removal of the -CO ligands, although the chemistry is still unknown. The reaction of carbonyl clusters with an elemental chalcogenide generates a variety of polynuclear compounds with a *d*-state coordination center [6–8]. It has been reported that polynuclear clusters such as Pt_n (where n is about 6) are small enough to be considered as quasi molecular metal clusters rather than metallic. Their catalytic properties are distinct from those of metallic particles. The chemisorption of small molecules on the surface and the following interface reaction are topics of considerable interest in catalysis and electrocatalysis. Transition-metal chalcogenide cluster compounds are of primary interest owing to the coordination of the oxygen to the transition metal complexes [9, 10] and to the bimetallic interactions giving rise to catalytic processes in the development of hydrodesulfurization reactions [11–13] and cathodes in batteries and fuel cells [14–16]. However, it has been reported that dichalcogenides of ruthenium have very low electrocatalytic activity for oxygen reduction in acid media [7]. The aim of this work is to investigate a ruthenium-sulfur-carbonyl cluster electrocatalyst, prepared by pyrolysis in a sealed ampoule at 300 °C, which presented good stability and electrocatalytic activity for molecular oxygen reduction in an acidic medium.

S. Durón (✉) · R. Rivera-Noriega
M.A. Leyva · O. Solorza-Feria
Depertamento de Química, CINVESTAV-IPN,
A. Postal 14-740, 07000 D.F., México

P. Nkeng · G. Poillerat
Labaratoire d'Electrochimie et de Chimie du Corps Solide,
Université Louis Pasteur, B.P. 296, 67008 Strasbourg, France

Experimental

Material synthesis

The syntheses of the $Ru_xS_y(CO)_n$ electrocatalysts were performed by mixing $Ru_3(CO)_{12}$ (Strem) and elemental sulfur (Aldrich) in a sealed glass ampoule. The mixture was then pyrolyzed at 300 °C for 24 h. The resulting powder was rinsed twice with a mixture of hexane, chloroform, and ethyl acetate in order to eliminate the non-reacting compound. Afterwards the compound was dried at 120 °C overnight. The resulting material was ground to a fine powder and used for electrochemical measurements and optical and structural characterizations.

Electrode preparation and electrochemical set-up

Oxygen reduction on $Ru_xS_y(CO)_n$ was studied using a rotating Pt ring-$Ru_xS_y(CO)_n$ disk electrode (RRDE). The disks were prepared

from five different syntheses, all the samples giving similar results. Thus 3 mg of the electrocatalyst was mixed with 3 mg of carbon paste (graphite from Aldrich and paraffin from Merck, mixed in a ratio of 2 : 1 w/w [17, 18]). The mixtures were back contacted with carbon paste and mounted on a Nylamid holder to obtain the disk electrode. The electrode surface was polished and rinsed with deionized water before used. To make the RRDE the disk holder was mounted on a concentric platinum ring electrode. A conventional three-compartment glass cell was used. The electrochemical measurements were performed with an EG&G bi-potentiostat and a Pine MSRX rotation speed controller. The collection efficiency, N, was determined to be 0.26 from the slope of I_R versus I_D at different rotation rates using 5×10^{-3} M $K_3Fe(CN)_6$ in 10^{-1} M K_2SO_4. The RRDE measurements for O_2 reduction were performed in a 0.5 M H_2SO_4 (pH 0.3) electrolyte. The reference electrode was a mercury sulfate electrode (MSE), Hg/Hg_2SO_4 in 0.5 M H_2SO_4 (MSE = 0.67 V/NHE). A platinum mesh was used as a counter electrode. All chemicals were used without further purification. The electrochemical experiments were done at room temperature (25 °C). The electrodes were activated in the oxygen purged electrolyte with argon, by scanning the potential in the region between 0.40 V/NHE and 0.10 V/NHE at 50 mV/s for 20 min. Thereafter, the electrolyte was saturated with pure oxygen and maintained on the electrolyte surface during the measurements. Hydrodynamic experiments were recorded in the rotation rate range of 100–1600 rpm at 5 mV/s. The ring potential was kept at 1.4 V/NHE, at wich all the H_2O_2 molecules that reached the ring were oxidized to O_2 [19, 20]. The ring current (I_R) was recorded simultaneously with the disk current (I_D).

Material characterization

Differential scanning calorimetry (DSC) was performed on an automated Perkin-Elmer DSC-7 calorimeter. Infrared spectra were obtained on a FT-IR Perkin-Elmer 16F spectrometer under PC control. X-ray diffraction (XRD) analysis was performed on a Siemens D5000 using Cu Kα monochromated radiation ($\lambda = 0.115478$ nm). Micrographs were recorded with a Jeol JSM-35CF electron microscope operating at 20 kV. The powder was fixed on an adhesive carbon tape.

Results and discussion

Figure 1 shows DSC curves obtained with the mixed reagents and the pure dodecacarbonyl triruthenium. The thermal response of $Ru_3(CO)_{12}$ (curve a), gave endothermic peaks at 162 °C, 255 °C and 290 °C. The peak observed at 162 °C is attributed to the $Ru_3(CO)_{12}$ fusion and the other two peaks are attributed to the decomposition of $Ru_3(CO)_{12}$ and its transformation to metallic ruthenium [23, 24]. Curve b in Fig. 1 depicts the calorimetric behavior of $Ru_3(CO)_{12}$ + elemental sulfur, yielding endothermic peaks at 130 °C and 165 °C, respectively, an exothermic peak at 230 °C and two more exothermic peaks around 450 °C. At 130 °C the sulfur is fused and at 165 °C the peak of the fusion with the $Ru_3(CO)_{12}$ is observed. The exothermic peak observed at 230 °C is attributed to the chemical reaction for the formation of the pyrolyzed product. The syntheses have been carried out at 300 °C and the thermal response of the pyrolysis product is shown in curve c. The prepared compound is stable below 380 °C but above this an exothermic peak appears, attributed to degradation of the product.

The XRD patterns of the ruthenium carbonyl used as the reagent, metallic ruthenium powder, ruthenium di-

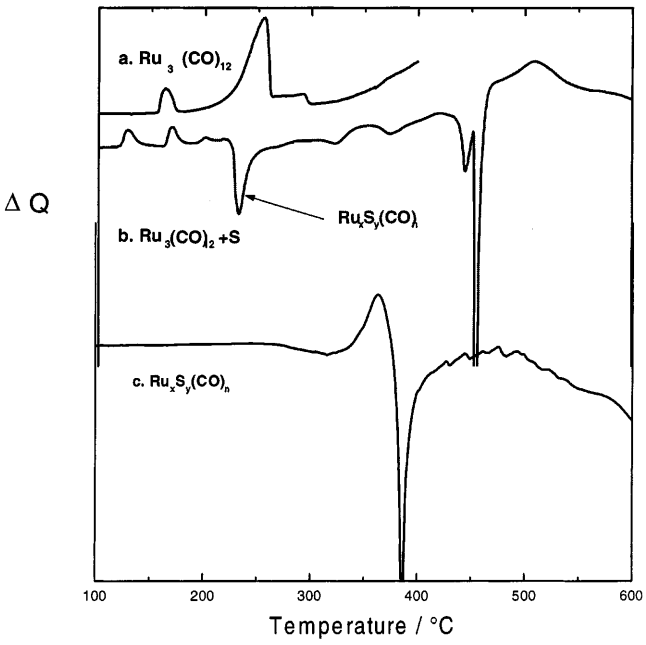

Fig. 1 Differential scanning calorimetry curves for *a* $Ru_3(CO)_{12}$, *b* $Ru_3(CO)_{12}$ + S, and *c* $Ru_xS_y(CO)_n$ powder synthesized by pyrolysis of $Ru_3(CO)_{12}$ and elemental sulfur at 300 °C

sulfide powder and the powders obtained from pyrolysis are presented in Fig. 2. In the 2θ range 0–60° no peaks are detected, indicating that the synthesized compound is either amorphous or poorly crystallized. Similar behavior was observed for transition metal chalcogenide compounds synthesized from a chemical precipitation reaction [21, 22].

SEM photographs of the synthesized product are shown in Fig. 3. The surface appears as small, near-spherical nodules, partially fused together with sizes particles between 1–10 μm. This type of morphology is typical of poorly crystallized chalcogenides prepared at low temperature. The energy dispersive X-ray (EDX) analyzer of the scanning electron microscope give a Ru/S atomic ratio of 1.65. The precise structure and real composition have not yet been determined owing to the insolubility and the amorphous character of the synthesized compound.

Figure 4 shows a FT-IR spectrum of a KBr pellet of the synthesized $Ru_xS_y(CO)_n$ electrocatalyst after (Fig. 4A) and before (Fig. 4B) washing with the mixture of solvents described above. In the region of 2100–1400 cm^{-1} appear two bands near 2000 cm^{-1}, attributed to terminal carbonyls. This result confirms that the -CO bonds to the metal centers are maintained and incorporated into the cluster compound [25].

RRDE experiments were performed on the Ru_xS_y-$(CO)_n$ electrocatalyst in order to measure the amount of hydrogen peroxide produced in the electrochemical oxygen reduction process. The current-potential curves of the RRDE experiments as a function of potential and rotating rate are depicted in Fig. 5. The equilibrium potential is

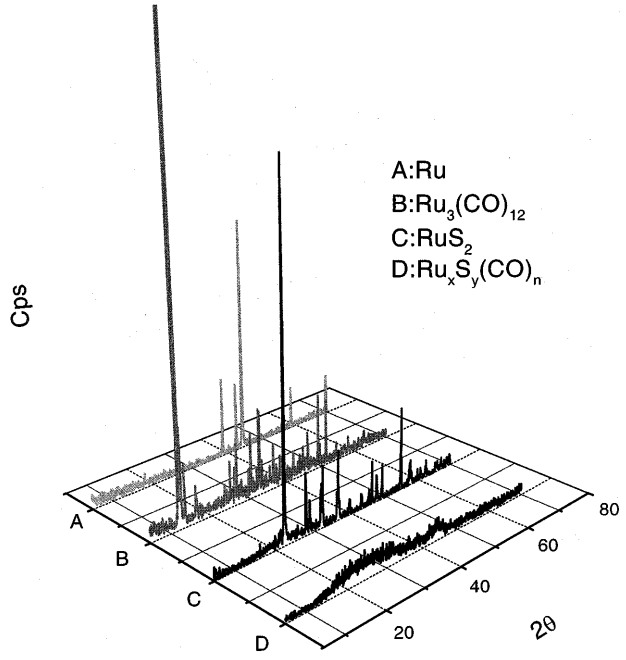

Fig. 2 X-ray diffraction patterns of *A* Ru (metallic powder), *B* $Ru_3(CO)_{12}$, *C* RuS_2 powder and *D* $Ru_xS_y(CO)_n$

about −0.82 V/NHE, from which the oxygen reduction current at the disk, I_D, begins. The hydrogen peroxide produced during the oxygen reduction could be detected and collected at the ring electrode. The ring current, I_R, observed in Fig. 5 shows a dependence on the rotation rate and a poor bell shape. It has been pointed out that the shape of the I_R curves depends strongly on the electrocatalyst properties and the kinetic mechanism [26, 27]; thus for some materials the classical bell shape can be absent [28, 29], and the curves as shown in Fig. 5 can be related to non-further-peroxide-reduction behavior [30, 31].

The percentage of hydrogen peroxide, $\%H_2O_2 = |I_R/N|/(|I_R/N| + I_D) \times 100$, produced as an intermediate in the oxygen reduction as a function of the electrode potential, is depicted in Fig. 6. A maximum of 5.5 ± 0.2% is observed at 0.31 V/NHE. This result demonstrated that the multi-electron charge transfer ($4e^-$) of oxygen reduction on the $Ru_xS_y(CO)_n$ electrocatalyst has a yield of more than 94% to water formation in 0.5 M H_2SO_4.

The reaction at the disk electrode seems to be under combined kinetic and diffusion control. The disk currents, covering the 0.82–0.55 V range, become independent of the angular frequency of rotation, ω. The range of the slowly increasing currents is broader as ω is increased, as expected for an electrochemical reaction under mixed control. At about 0.30 V, mass transport kinetic contributions become significant. The height of the cathodic current between 0.05 and 0.30 V increases with the rotation rate. The O_2 reduction kinetics are often assumed to be first order with respect to the reactant in all reaction steps. To prove this condition, the linearity of i^{-1} against $\omega^{-1/2}$ is established. For a first reaction order with respect to dissolved oxygen the disk current density i_D is related to ω by the expression [32]:

$$\frac{1}{i_D} = \frac{1}{i_k} + \frac{1}{B\omega^{1/2}} \tag{1}$$

where i_k is the kinetic current density for O_2 reduction, $\omega = 2\pi f$, with f being the frequency of electrode rotation, and B, which is related to diffusion limiting current i_d by the expression $i_d = B\omega^{1/2}$, is given by [32]:

$$B = 0.62nFD^{2/3}\nu^{-1/6}C_{O_2} \tag{2}$$

where n is the number of transferred electrons in the overall reduction process, F is the Faraday constant (a value of 96 490 C mol^{-1} was taken in calculations), D is

Fig. 3 Scanning electron micrography of $Ru_xS_y(CO)_n$ synthesized at 300 °C

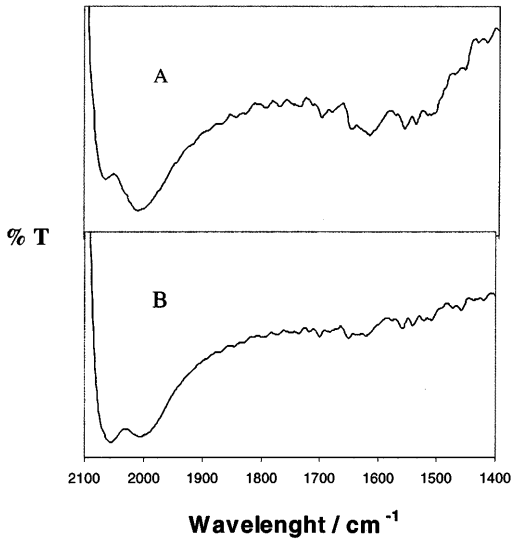

Fig. 4 Fourier transform infrared spectra of $Ru_xS_y(CO)_n$ in a KBr pellet in the 2100–1400 cm^{-1} region

the diffusion coefficient of the molecular O_2 in 0.5 M sulfuric acid (1.4×10^{-5} cm^2 s^{-1} [33]), v is the kinematic viscosity (0.01 cm^2 s^{-1}), and C_{O_2} is the concentration of molecular oxygen (1.1×10^{-6} mol cm^{-3} [33]). A typical i^{-1} against $\omega^{-1/2}$ plot is shown in Fig. 7. At high polarizations, the slopes over the wide frequency intervals can be fitted with that calculated for behavior with $n = 4$. This confirmed the results assessed with RRDE, where the oxygen reduction proceeded by an overall four-electron transfer process, i.e. $O_2 + 4H^+ + 4e^- \rightarrow 2H_2O$.

Figure 8 shows the mass-transfer-corrected Tafel plot of the disk current of Fig. 5. At low polarization a linear region is determined with a Tafel slope, b_{lp}, of -0.124 ± 0.002 V dec^{-1}, ranging from 0.80 to 0.68 V. Meanwhile, at high polarization a Tafel slope, b_{hp}, of -0.254 ± 0.003 V is determined. This means a transfer coefficient value of $\alpha = 0.48$ for the O_2 reduction in 0.5 M H_2SO_4 at 25 °C, at the low potential range.

Although it is difficult to determine the reaction mechanism by means of only Tafel parameters, the slope here obtained is close to the value of $2RT/F$ found for a slow discharge of an electron step [34]. At low overpotentials it is possible to assume that the rate determining step in the O_2 reduction must be the electroreduction of adsorbed oxygen, $(O_2)_{ads}$, i.e. $(O_2)_{ads} + e^- \rightarrow (O_2^-)_{ads}$, as has been described before for transition metals in acid medium [35, 36].

Slopes with values larger than -0.120 V dec^{-1} are attributed to mixed carbonyl compounds with low and high nuclearity formed during the pyrolysis, which interact on the surface with the adsorbed oxygen and change the kinetics in the region of high polarization. Another explanation of the high value of b_{hp} could be that the many O_2^- adsorbed ions and H_2O molecules around the electrical double layer hinder the oxygen adsorption/electron transfer and possibly change the oxygen reduction pathway.

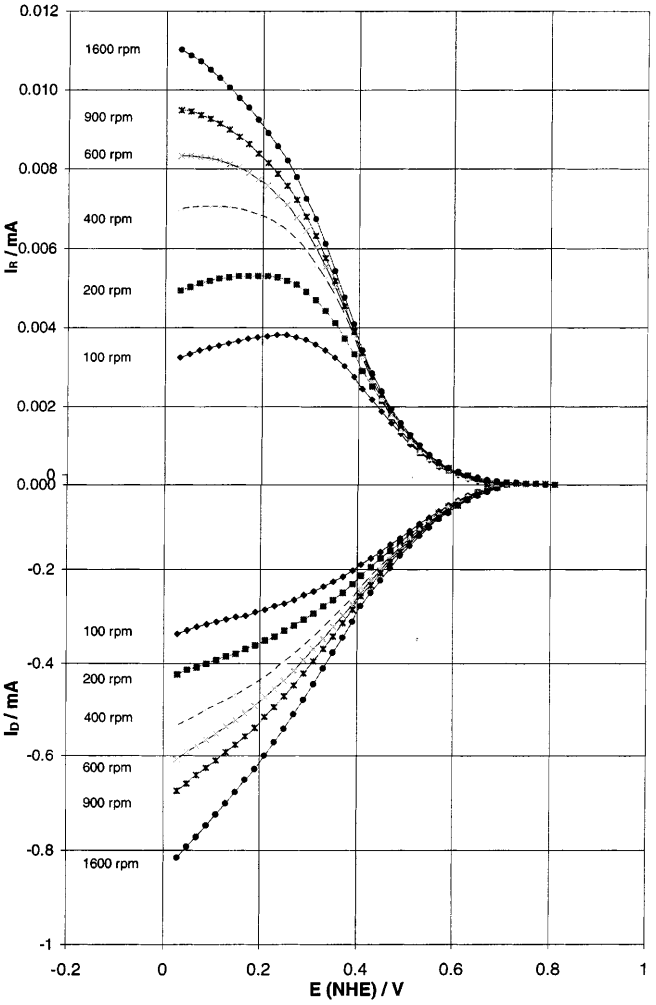

Fig. 5 Current-potential curves for $Ru_xS_y(CO)_n$ disk and Pt ring electrodes in a 0.5 M H_2SO_4 solution saturated with oxygen at different rotating rates. The disk potential was swept from −0.82 to −0.05 V vs. NHE and the ring potential was set at 1.4 V/NHE. Scan rate: 5 mV s^{-1}

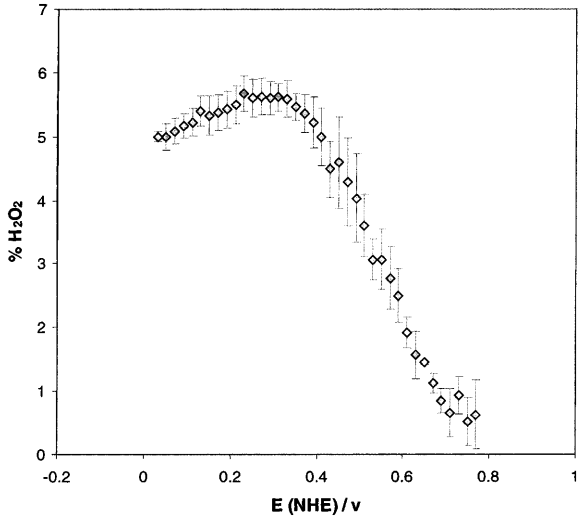

Fig. 6 Percentage of H_2O_2 produced on the reduction of O_2 on $Ru_xS_y(CO)_n$ electrocatalyst

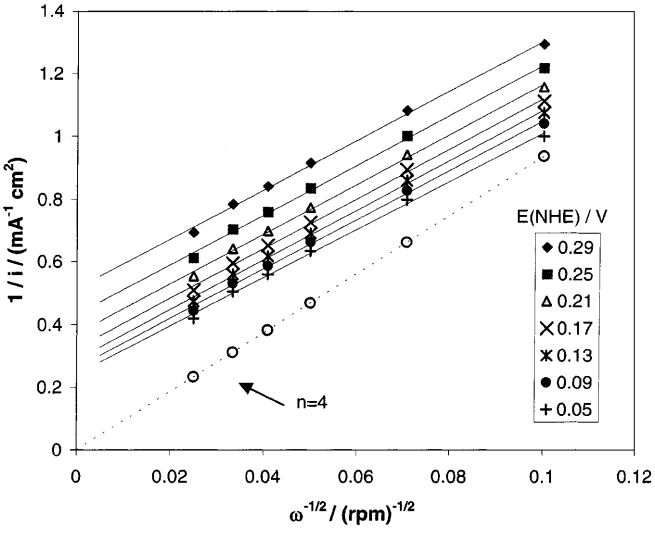

Fig. 7 Koutecky-Levich plots for the $Ru_xS_y(CO)_n$ electrocatalyzed reduction of molecular oxygen

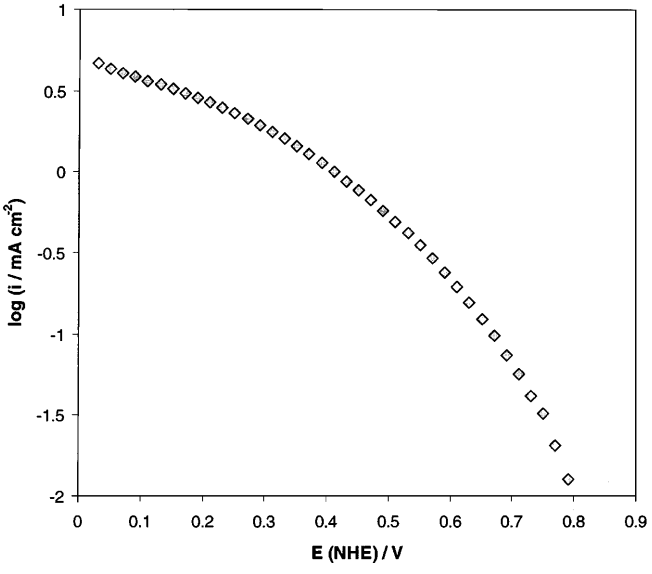

Fig. 8 Mass transfer corrected Tafel plot for the molecular reduction of oxygen in 0.5 M H_2SO_4 at 25 °C

Conclusions

A ruthenium-sulfur-carbonyl cluster compound, $Ru_xS_y(CO)_n$, has been prepared by pyrolysis at 300 °C for 24 h, although additional work is needed to determine the chemical composition, structure and properties with precision. The morphology of the produced electrocatalyst is typical of a poorly crystallized chalcogenide prepared at low temperature, with particle sizes of the order of micrometers. The electrochemical study showed reactions having first-order kinetics with respect to dissolved O_2 and a multi-electron charge reaction for the reduction of oxygen to water (i.e., $O_2 + 4H^+ + 4e^- \rightarrow 2H_2O$).

Acknowledgements The authors gratefully acknowledged the support provided by ECOS (M97E05). S.D. thanks the Consejo Nacional de Ciencia y Tecnologia (CONACYT) for a thesis scholarship.

References

1. Deeming AJ (1995) Trinuclear clusters of ruthenium and osmium: (i) Introduction and simple neutral, anionic and hydrido clusters. In: Shriver DF, Bruce MI (eds) Comprehensive organometallic chemistry II, vol. 7. Pergamon, Oxford, p 684
2. Wong WT (1998) J Chem Soc Dalton Trans 1253
3. Bond AM, Colton R (1997) Coord Chem Rev 166: 161
4. Shriver DF, Kaesz HD, Adams RD (1990) The chemistry of metal cluster complexes. VCH, New York, p 11
5. Somorjai GA (1995) Surf Sci 335: 10
6. Lin Z, Fan M-F (1997) Structural and electronic paradigms in cluster chemistry (1997) Springer, Berlin Heidelberg New York, pp 36–80
7. Alonso-Vante N Tributsch H (1994) Electrode materials and strategies for photoelectrochemistry. In: Lipkowski J, Ross PN (eds) Electrochemistry of novel materials, vol. III. VCH, New York, p 1
8. Adams RD (1985) Polyhedron 4: 2003
9. Tavagnacco C, Moszner M, Cozzi S, Peressini S, Costa G (1998) J Electroanal Chem 448: 41
10. Shi C, Steiger B, Anson FC (1995) Pure Appl Chem 67: 319
11. Riaz U, Curnow OJ, Curtis MD (1994) J Am Chem Soc 116: 4357
12. Muetterties EL, Krause MJ (1983) Angew Chem Int Ed Engl 22: 135
13. Gates BC (1995) Chem Rev 95: 511
14. Kordesh KV, Simader GR (1995) Chem Rev 95: 191
15. Blomen L, Mugerwa GR (1993) Fuel Cell Systems, Plenum Press, New York
16. Solorza-Feria O, Ramirez-Raya S, Rivera-Noriega R, Fernandez-Valverde M (1997) Thin Solid Films 311: 164
17. Alonso-Vante N, Schubert B, Tributsch H (1989) Mat chem Phys 22: 281
18. McCreery RL (1991) Carbon electrodes: structural effects on electron transfer kinetics. In: Bard AJ (ed) Electroanalytical chemistry, vol 17. Dekker, New York, p 221
19. Genshaw MA, Damjanovic A, Bockris JO'M (1967) J Electroanal Chem 15: 163
20. Bockris JO'M, Srinivasan S (1966) J Electroanal Chem 11: 350
21. Castellanos RH, Campero A, Solorza-Feria O (1998) Int J Hydrogen Energy 23: 4311
22. Trapp V, Christensen P, Hamnett A (1996) J Chem Soc Faraday Trans 92: 4311
23. Banditelli P, Cuccuru A, Sodi F (1976) Thermochim Acta 16: 89
24. Battiston GA, Bor G, Dietler UK, Kettle SFA, Rossetti R, Sbrignadello G, Stanghellini PL (1980) Inorg Chem 19: 1961
25. Psaro R, Fusi A, Ugo R, Basset JM, Smith AK, Hugues F (1980) J Mol Catal 7: 511
26. Fischer P, Heitbaum J (1980) Electroanal Chem 112: 231
27. Schubert B, Gocke E, Schöllhorn R, Alonso-Vante N, Tributsch H (1996) Electrochim Acta 41: 1471
28. Zurilla RW, Sen RK, Yeager E (1978) J Electrochem Soc 125: 1103
29. Steiger B, Anson FC (1994) Inorg Chem 33: 5767
30. Bockris JO'M, Khan SU (1993) Surface electrochemistry. Plenum Press, New York, p 328
31. Damjanovic A, Genshaw MA, Bockris JO'M (1966) J Chem Phys 45: 4057
32. Pleskov YV, Filinovskii VY (1976) The rotating disk electrode. Plenum Press, New York
33. Hsueh K, Gonzalez E, Srinivasan S (1983) Electrochim Acta 28: 691
34. Bockris JO'M (1956) J Chem Phys 24: 817
35. Hoare JP (1965) J Electrochem Soc 112: 602
36. Gnanamuthu DS, Petrocelli JV (1967) J Electrochem Soc 114: 1036